

Aharonov–Bohm effect for a fermion field in a planar black hole “spacetime”

M. A. Anacleto^{1,a}, F. A. Brito^{1,2,b}, A. Mohammadi^{1,c}, E. Passos^{1,3,d}

¹ Departamento de Física, Universidade Federal de Campina Grande, Caixa Postal 10071, Campina Grande, Paraíba 58429-900, Brazil

² Departamento de Física, Universidade Federal da Paraíba, Caixa Postal 5008, João Pessoa, Paraíba 58051-970, Brazil

³ Instituto de Física, Universidade Federal do Rio de Janeiro, Caixa Postal 21945, Rio de Janeiro, Brazil

Received: 7 March 2017 / Accepted: 31 March 2017 / Published online: 12 April 2017

© The Author(s) 2017. This article is an open access publication

Abstract In this paper we consider the dynamics of a massive spinor field in the background of the acoustic black hole spacetime. Although this effective metric is acoustic and describes the propagation of sound waves, it can be considered as a toy model for the gravitational black hole. In this manner, we study the properties of the dynamics of the fermion field in this “gravitational” rotating black hole as well as the vortex background. We compute the differential cross section through the use of the partial wave approach and show that an effect similar to the gravitational Aharonov–Bohm effect occurs for the massive fermion field moving in this effective metric. We discuss the limiting cases and compare the results with the massless scalar field case.

1 Introduction

Unruh [1, 2] in 1981 suggested a theoretical method based on the fact that, considering the sound wave motion, a change of a subsonic runoff for supersonic flow forms an event horizon analogous to an event horizon of a gravitational black hole. Since then, the study of analog models of gravity [3–19] has become an important field where one investigates the Hawking radiation as well as to improve the theoretical understanding of quantum gravity. For such analog models there are many examples, so we highlight gravity waves [20], water [21], slow light [22–24], optical fibers [25] and electromagnetic waveguides [26]. Specially in fluid systems, the propagation of perturbations of the fluid has been analyzed in many analog models of acoustic black holes, such as the models of superfluid helium II [27], atomic Bose–Einstein

condensates [28, 29] and one-dimensional Fermi degenerate noninteracting gas [30] that were elaborated to create a sonic black hole geometry in the laboratory. More specifically, in a quantum liquid the quasiparticles are bosons (phonons) in ⁴He and bosons and fermions in ³He which move in the background of effective gauge and/or gravity simulated by the dynamics of collective modes. These quasiparticles are analogs of elementary particles of low-energy effective quantum field theory. In particular, phonons propagating in the inhomogeneous liquid can be described by the effective lagrangian mimicking the dynamics of a scalar field in the curved spacetime given by the effective acoustic metric where the free quasiparticles move along geodesics. In superfluid ³He-A, the effective quantum field theory contains chiral fermion quasiparticles where the collective bosonic modes interact with these elementary particles as gauge fields and gravity. These advances are important for a better insight into the understanding of quantum gravity. In addition, the study of a relativistic version of acoustic black holes was presented in [31–34]. Furthermore, the acoustic black hole metrics obtained from a relativistic fluid in a noncommutative spacetime [35] and Lorentz-violating Abelian Higgs model [36, 37] have been considered. The thermodynamics of acoustic black holes in two dimensions was studied in [38]. The authors in [39–41] studied acoustic black holes in the framework of neo-Newtonian hydrodynamics and in [42] the effect of neo-Newtonian hydrodynamics on the super-resonance phenomenon was analyzed.

In 1959, Aharonov and Bohm showed that when the wave function of a charged particle passing around a region with the magnetic flux, despite the magnetic field being negligible in the region through which the particle passes, experiences a phase shift as a result of the enclosed magnetic field [43]. The Aharonov–Bohm (AB) effect, which is essentially the scattering of charged particles, has been used to address several issues in planar physics and it was experimentally confirmed

^a e-mail: anacleto@df.ufcg.edu.br

^b e-mail: fabrito@df.ufcg.edu.br

^c e-mail: a.mohammadi@fisica.ufpb.br

^d e-mail: passos@df.ufcg.edu.br

by Tonomura [44] – for a review see [45]. The effect can also be simulated in quantum field theory as for example by using a nonrelativistic field theory for bosonic particles which interact with a Chern–Simons field [46]. More specifically, in [47–50] was addressed the AB effect considering the noncommutative spacetime and in [51] the effect was obtained due to violation of Lorentz symmetry in quantum field theory.

Furthermore, several other analogs of the AB effect were found in gravitation [52–56], fluid dynamics [57,58], optics [61] and Bose–Einstein condensates [62,63]. In [57] it was shown that the background flow velocity \vec{v} plays the role of the electromagnetic potential \vec{A} , and the integrated vorticity in the core $\Omega = \int (\vec{\nabla} \times \vec{v}) \cdot d\vec{S}$ plays the role of the magnetic flux $\Phi = \int \vec{B} \cdot d\vec{S}$. Thus, surface waves on water crossing an irrotational (bathtub) vortex experience an analog of the AB effect. Also, the gravitational analog of the electromagnetic AB effect which is purely classical is related to the particles constrained to move in a region where the Riemann curvature tensor vanishes. However, a gravitational effect arises from a region of nonzero curvature from which the particles are excluded.

An interesting system was investigated in [64], where it was shown that planar waves scattered by a draining bathtub vortex develops a modified AB effect that has a dependence on two dimensionless parameters, related to the circulation and draining rates [65]. It has been found an inherent asymmetry even in the low-frequency regime which leads to novel interference patterns. More recently in [66–68], the analysis made in [64] was extended to a Lorentz-violating and non-commutative background [69–75], which allows the system to have persistence of phase shifts even if circulation and draining vanish.

One of the theoretical methods of investigating the underlying structure of the spacetime is studying the solution of field equations for the fermion fields, besides the bosonic ones, in a curved geometry. The behavior of matter fields in the vicinity of black holes results in the better understanding of their properties. Fermion fields were analyzed in a Kerr black hole, in the near horizon limit, as well as in the case of Reissner–Nordström black hole [76,77]. In [78] nonzero Dirac fermion modes in the spacetime of a black hole cosmic string system was considered. The authors studied the near-horizon behavior of fermion fields which results in superconductivity in the case of extremal charged dilaton black hole.

Although the effective sonic black hole spacetime is not the one fermion fields would observe, but it can be used as a toy model and a mathematical tool to study and as a result understand better the dynamics of the massive and massless fermion fields in a gravitational rotating black hole as well as a vortex background and shed light on the underlying physics. In the present study we consider the dynamics

of a massive Dirac spinor field in a curved spacetime and apply the acoustic black hole metric to obtain the differential cross section for scattered planar waves which leads to an analog AB effect. Besides that, we compare the results with the massless scalar field case.

The paper is organized as follows. In Sect. 2 we briefly introduce the acoustic black hole. In Sect. 3 we compute the differential cross section due to the scattering of planar waves that leads to an analog AB effect. Finally in Sect. 4 we present our final considerations.

2 Acoustic black hole

The acoustic line element in polar coordinates is governed by

$$ds^2 = (c^2 - v^2)dt^2 + 2(v_r dr + v_\phi d\phi)dt - dr^2 - r^2 d\phi^2, \tag{1}$$

where $c = \sqrt{d\hbar/d\rho}$ is the velocity of sound in the fluid and v is the flow/fluid velocity. We consider the flow with the velocity potential $\psi(r, \phi) = D \ln r + C\phi$ whose flow/fluid velocity is given by

$$\vec{v} = -\frac{D}{r}\hat{r} + \frac{C}{r}\hat{\phi}, \tag{2}$$

Thus, Eq. (1) can be rewritten as follows:

$$ds^2 = \left(c^2 - \frac{C^2 + D^2}{r^2}\right) dt^2 + 2\left(\frac{C}{r} d\phi - \frac{D}{r} dr\right) dt - dr^2 - r^2 d\phi^2, \tag{3}$$

where C and D are the constants of the circulation and draining rates of the fluid flow. The radius of the ergosphere given by $g_{00}(r_e) = 0$, and the horizon, the coordinate singularity, given by $g_{rr}(r_h) = 0$, are

$$r_e = \frac{\sqrt{C^2 + D^2}}{c}, \quad r_h = \frac{|D|}{c}. \tag{4}$$

We set $c = 1$, and choose the following change of variables [64]:

$$d\tilde{t} = dt - \frac{D}{rf(r)}dr, \quad d\tilde{\phi} = d\phi - \frac{CD}{r^3 f(r)}dr, \tag{5}$$

where $f(r) = 1 - D^2/r^2$, and which results in the following line element:

$$ds^2 = \left[f(r) - \frac{C^2}{r^2}\right] d\tilde{t}^2 - \frac{dr^2}{f(r)} - r^2 d\tilde{\phi}^2 + C \left(d\tilde{t} d\tilde{\phi} + d\tilde{\phi} d\tilde{t}\right). \tag{6}$$

Therefore, the metric can be written in the form

$$g_{\mu\nu} = \begin{pmatrix} f(r) - C^2/r^2 & 0 & C \\ 0 & -f^{-1}(r) & 0 \\ C & 0 & -r^2 \end{pmatrix}, \tag{7}$$

with the inverse $g^{\mu\nu}$

$$g^{\mu\nu} = \begin{pmatrix} f^{-1}(r) & 0 & Cf^{-1}(r)/r^2 \\ 0 & -f(r) & 0 \\ Cf^{-1}(r)/r^2 & 0 & -r^{-2} + C^2f^{-1}(r)/r^4 \end{pmatrix}. \tag{8}$$

We know that this effective metric is acoustic which describes the propagation of sound waves. It is trivial that the Dirac field does not obey the acoustic metric. In the case it exists in the considered media, it would have its own metric with its own ‘‘speed of light’’. We are interested in the dynamics of the fermion field in this background as a toy model to investigate the physical properties in contrast with the scalar field case. In the following, we study the scattering of monochromatic planar waves of frequency ω for a massive fermion by the draining vortex, a process governed by two key quantities; circulation and draining.

3 Fermion field in the acoustic black hole background

Now let us consider a spinor field in the background of the sonic black hole. The dynamics of a massive spinor field in curved spacetime is described by the Dirac equation

$$(i\gamma^\mu \mathcal{D}_\mu - M_f)\psi = 0, \tag{9}$$

where $\mathcal{D}_\mu = \partial_\mu + \Gamma_\mu$, γ^μ are the Dirac matrices in curved spacetime and Γ_μ are the spin connections. Let us choose the following representation:

$$\gamma^{(0)} = \sigma^3, \quad \gamma^{(1)} = i\sigma^2, \quad \gamma^{(2)} = -i\sigma^1. \tag{10}$$

For the geometry at hand, using the relation $\gamma^\mu = e^\mu_{(a)}\gamma^{(a)}$, the gamma matrices take the form

$$\begin{aligned} \gamma^0 &= \frac{1}{\sqrt{f}}\sigma^3, \quad \gamma^1 = i\sqrt{f}(\sin\phi\sigma^1 + \cos\phi\sigma^2), \\ \gamma^2 &= \frac{C}{r^2\sqrt{f}}\sigma^3 + \frac{i}{r}(\sin\phi\sigma^2 - \cos\phi\sigma^1). \end{aligned} \tag{11}$$

One can find the triad coordinate using $e^\mu_{(a)}e^{\nu}_{(b)}\eta^{ab} = g^{\mu\nu}$ as

$$e^\mu_{(a)} = \begin{pmatrix} \frac{1}{\sqrt{f}} & 0 & \frac{C}{r^2\sqrt{f}} \\ 0 & \sqrt{f}\cos\phi & \sin\phi/r \\ 0 & -\sqrt{f}\sin\phi & \cos\phi/r \end{pmatrix}, \tag{12}$$

where

$$\eta^{ab} = \begin{pmatrix} 1 & 0 & 0 \\ 0 & -1 & 0 \\ 0 & 0 & -1 \end{pmatrix}. \tag{13}$$

The only nonzero Christoffel symbols are

$$\begin{aligned} \Gamma_{01}^0 &= \Gamma_{10}^0 = \frac{C^2+D^2}{r^3f}, & \Gamma_{00}^1 &= \frac{C^2+D^2}{r^3}f, \\ \Gamma_{12}^0 &= \Gamma_{21}^0 = -\frac{C}{rf}, & \Gamma_{11}^1 &= -\frac{D^2}{r^3f}, \\ \Gamma_{01}^2 &= \Gamma_{10}^2 = \frac{C(C^2+D^2)}{r^5f}, & \Gamma_{22}^1 &= -rf, \\ \Gamma_{12}^2 &= \Gamma_{21}^2 = \frac{1}{r} - \frac{C^2}{r^3f}. \end{aligned}$$

Now, using

$$\Gamma_\mu = \frac{1}{4}\gamma^{(a)}\gamma^{(b)}e^{\nu}_{(a)}\nabla_\mu e_{(b)\nu}, \tag{14}$$

one can find the spin connection components for the system as follows:

$$\begin{aligned} \Gamma_0 &= \frac{C^2 + D^2}{2r^3} (\cos\phi\sigma^1 - \sin\phi\sigma^2), \\ \Gamma_1 &= -\frac{C}{2r^2\sqrt{f}} (\cos\phi\sigma^2 + \sin\phi\sigma^1), \\ \Gamma_2 &= -\frac{i}{2} (1 + \sqrt{f})\sigma^3 - \frac{C}{2r} (\cos\phi\sigma^1 - \sin\phi\sigma^2). \end{aligned} \tag{15}$$

In the Dirac equation there appears

$$\begin{aligned} \gamma^\mu \Gamma_\mu &= i \left(\frac{D^2}{2r^3\sqrt{f}} + \frac{(1 + \sqrt{f})}{2r} \right) (\cos\phi\sigma^2 + \sin\phi\sigma^1) \\ &\quad - i \frac{C(1 + \sqrt{f})}{2r^2\sqrt{f}}. \end{aligned} \tag{16}$$

Now, we substitute the following spinor field in the Dirac equation:

$$\psi = \begin{pmatrix} \psi_1 e^{i\phi/2} \\ \psi_2 e^{-i\phi/2} \end{pmatrix} e^{-i\omega t + ij\phi}, \tag{17}$$

where $j = \pm 1/2, \pm 3/2, \dots$. Replacing the corresponding parameters in the Dirac equation, we obtain

$$\begin{aligned} \left[\frac{\omega}{\sqrt{f}} - \frac{C}{r^2} \left(\frac{j}{\sqrt{f}} - 1/2 \right) - M_f \right] \psi_1 \\ + i \left[\sqrt{f}\partial_r + \frac{(j-1/2)}{r} + \left(\frac{D^2}{2r^3\sqrt{f}} + \frac{(1+\sqrt{f})}{2r} \right) \right] \psi_2 = 0, \end{aligned} \tag{18}$$

$$\begin{aligned} \left[\frac{\omega}{\sqrt{f}} - \frac{C}{r^2} \left(\frac{j}{\sqrt{f}} + 1/2 \right) + M_f \right] \psi_2 \\ + i \left[\sqrt{f}\partial_r - \frac{(j+1/2)}{r} + \left(\frac{D^2}{2r^3\sqrt{f}} + \frac{(1+\sqrt{f})}{2r} \right) \right] \psi_1 = 0. \end{aligned} \tag{19}$$

After decoupling the above equations for ψ_1 and ψ_2 and considering the change of variables as $\chi_1 = \sqrt{r} \psi_1$ and $\chi_2 = \sqrt{r} \psi_2$, we get

$$\frac{d^2 \chi_1}{d\rho_1^2} + \left[\lambda^2 + \frac{1/4 - \tilde{n}^2}{\rho_1^2} + \mathcal{O}\left[\frac{1}{\rho_1^4}\right] \right] \chi_1 = 0, \tag{20}$$

$$\frac{d^2 \chi_2}{d\rho_2^2} + \left[\lambda^2 + \frac{1/4 - \tilde{m}^2}{\rho_2^2} + \mathcal{O}\left[\frac{1}{\rho_2^4}\right] \right] \chi_2 = 0, \tag{21}$$

written as a power series in $1/\rho_1$ and in $1/\rho_2$, with $\lambda^2 = \omega^2 - M_f^2$, $m = j + 1/2$, $n = j - 1/2$ and

$$\tilde{n}^2 = n^2 - C(-\omega + M_f - 2n\omega) - D^2(\omega^2 + \lambda^2), \tag{22}$$

$$\tilde{m}^2 = m^2 - C(\omega + M_f - 2m\omega) - D^2(\omega^2 + \lambda^2). \tag{23}$$

In Eqs. (20) and (21), ρ_1 and ρ_2 are

$$\rho_1 = r + \frac{-2Cm + D^2(3\omega + 2M_f)}{2(\omega + M_f)r} + \mathcal{O}\left[\frac{1}{r^3}\right], \tag{24}$$

$$\rho_2 = r + \frac{2C - 2Cm + D^2(3\omega - 2M_f)}{2(\omega - M_f)r} + \mathcal{O}\left[\frac{1}{r^3}\right]. \tag{25}$$

Choosing $\alpha = C\omega$, $\beta = CM_f$ and $\gamma^2 = D^2(\omega^2 + \lambda^2)$, we have

$$\tilde{n}^2 = n^2 + 2\alpha n + (\alpha - \beta) - \gamma^2, \tag{26}$$

$$\tilde{m}^2 = m^2 + 2\alpha m - (\alpha + \beta) - \gamma^2. \tag{27}$$

Therefore for large r , ignoring the terms $\mathcal{O}[\frac{1}{\rho_1^4}]$ and $\mathcal{O}[\frac{1}{\rho_2^4}]$, one can obtain analytic solutions

$$\chi_1 = J_{\tilde{n}}(\lambda\rho_1), \tag{28}$$

$$\chi_2 = J_{\tilde{m}}(\lambda\rho_2). \tag{29}$$

In the limit $r \rightarrow \infty$, these two solutions converge to

$$\chi_1 = J_{\tilde{n}}(\lambda r), \tag{30}$$

$$\chi_2 = J_{\tilde{m}}(\lambda r). \tag{31}$$

It is not difficult to show numerically that these solutions besides satisfying the second order Eqs. (20) and (21), satisfy the first order Eqs. (18) and (19) in the limit $r \rightarrow \infty$. Comparing this result with the one in the Minkowski space, we obtain the following approximate expressions for the phase shift for the upper and lower components of the spinor fields:

$$\delta_u = \frac{\pi}{2}(n - \tilde{n}), \tag{32}$$

$$\delta_d = \frac{\pi}{2}(m - \tilde{m}), \tag{33}$$

where $n = m - 1$. For $|n|, |m| \gg \sqrt{\alpha + \alpha^2 + \beta + \gamma^2}$, one can expand the above expressions. Thus, we obtain

$$\delta_u = \frac{n}{|n|} \left[-\frac{\pi\alpha}{2} + \frac{\pi[-\alpha + \alpha^2 + \beta + \gamma^2]}{4n} - \frac{\pi\alpha[-\alpha + \alpha^2 + \beta + \gamma^2]}{4n^2} + \mathcal{O}\left[\frac{1}{n^3}\right] \right], \tag{34}$$

$$\delta_d = \frac{m}{|m|} \left[-\frac{\pi\alpha}{2} + \frac{\pi[\alpha + \alpha^2 + \beta + \gamma^2]}{4m} - \frac{\pi\alpha[\alpha + \alpha^2 + \beta + \gamma^2]}{4m^2} + \mathcal{O}\left[\frac{1}{m^3}\right] \right]. \tag{35}$$

The first term in both expressions, the dominant contribution, is exactly the same as the bosonic case considered in [64].

Now we can calculate the differential scattering cross section, which is given by

$$\frac{d\sigma}{d\phi} = |f_\omega(\phi)|^2, \tag{36}$$

where

$$f_\omega(\phi) = \sqrt{\frac{1}{2i\pi\lambda}} \sum_{m=-\infty}^{+\infty} (e^{2i\delta_m} - 1)e^{im\phi}. \tag{37}$$

For the δ_m when $m = 0$ one needs to use Eqs. (32)–(33). Therefore, the differential scattering cross section at long wavelengths, $\sqrt{\alpha + \alpha^2 + \beta + \gamma^2} \ll 1$, for a massive fermion in the acoustic black hole background is given as follows:

$$\begin{aligned} \frac{d\sigma_{\alpha \geq \beta + \gamma^2}}{d\phi} &= \frac{1}{2} \left(\frac{d\sigma_u}{d\phi} + \frac{d\sigma_d}{d\phi} \right) = \frac{\pi}{4\lambda \sin^2\left(\frac{\phi}{2}\right)} \left[\left(\alpha \cos\left(\frac{\phi}{2}\right) - \sqrt{\alpha + \beta + \gamma^2} \sin\left(\frac{\phi}{2}\right) \right)^2 \right. \\ &\quad \left. - \left(\alpha \cos\left(\frac{\phi}{2}\right) - \sqrt{-\alpha + \beta + \gamma^2} \sin\left(\frac{\phi}{2}\right) \right) \right. \\ &\quad \left. \times \left(\alpha \cos\left(\frac{\phi}{2}\right) \pm \sqrt{-\alpha + \beta + \gamma^2} \sin\left(\frac{\phi}{2}\right) \right) \right]. \end{aligned} \tag{38}$$

Obviously, in the case $\alpha = \beta + \gamma^2$ the two expressions for $\alpha > \beta + \gamma^2$ and $\alpha < \beta + \gamma^2$ are the same. In the absence of the circulation, the differential scattering cross section reduces to

$$\frac{d\sigma}{d\phi} = \frac{\pi(\beta + \gamma^2)}{2\lambda}, \tag{39}$$

which is ϕ independent. This is an expected result, since in the absence of the circulation the only term that con-

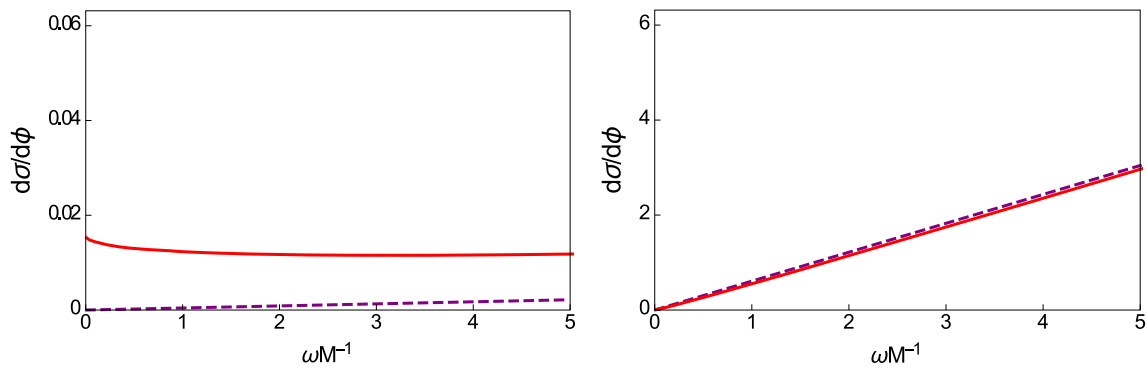


Fig. 1 $\frac{d\sigma}{d\phi}$ as a function of ωM^{-1} for two different values $\phi = \pi/5$ (left panel) and $\phi = \pi/100$ (right panel). The graphs are plotted for $C = 0.01M^{-1}$, $D = 0.01M^{-1}$ and $M_f = 0$. The solid (dashed) line represents the result for the fermionic (bosonic) case

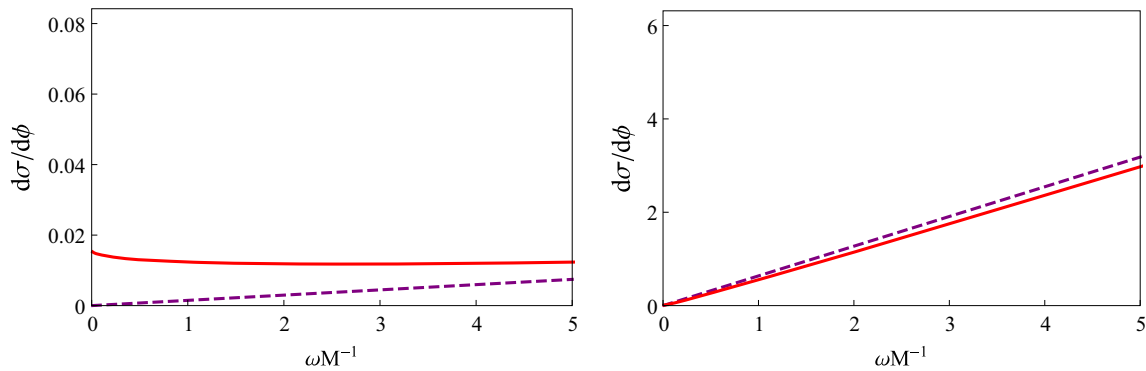


Fig. 2 $\frac{d\sigma}{d\phi}$ as a function of ωM^{-1} for two different values $\phi = \pi/5$ (left panel) and $\phi = \pi/100$ (right panel). The graphs are plotted for $C = 0.01M^{-1}$, $D = 0$ and $M_f = 0$. The solid (dashed) line represents the result for the fermionic (bosonic) case

tributes in the long wavelength regime to the differential cross section is $m = 0$, polar symmetric term. The same happens for the bosonic case which is equal to $\pi D^2\omega$. In the absence of the circulation, the result for the fermionic case is exactly the same as the bosonic one in the zero mass limit. The above expression vanishes when the draining is also zero. This is also an expected result, because without circulation and draining there is no source for the scattering and we should recover the Minkowski result.

Expanding the expression for the differential scattering cross section in Eq. (38) for small angles results in

$$\frac{d\sigma_{\alpha > \beta + \gamma^2}}{d\phi} = \frac{2\pi\alpha^2}{\lambda\phi^2} - \frac{\pi\alpha\sqrt{\alpha + \beta + \gamma^2}}{\lambda\phi} + \mathcal{O}[\phi^0], \quad (40)$$

$$\frac{d\sigma_{\alpha < \beta + \gamma^2}}{d\phi} = \frac{2\pi\alpha^2}{\lambda\phi^2} - \frac{\pi\alpha(\sqrt{\alpha + \beta + \gamma^2} + \sqrt{-\alpha + \beta + \gamma^2})}{\lambda\phi} + \mathcal{O}[\phi^0]. \quad (41)$$

Therefore, for $\phi \rightarrow 0$ and small α the dominant term in the differential scattering cross section is the first term in the above expression. It means that for small angles the circulation plays more important role compared to the draining.

Using $\alpha = C\omega$ and $\lambda = (\omega^2 - M_f^2)^{1/2}$, the first term in the above expression can be expanded as

$$\frac{d\sigma}{d\phi} = \frac{2\pi C^2\omega}{\phi^2} \left(1 + \frac{M_f^2}{2\omega^2} + \mathcal{O}[M_f^4/\omega^4] \right), \quad (42)$$

for small M_f/ω . The first term which is the result for massless fermion, matches exactly the one for the massless boson case.

Now one can compare the results for the fermionic and bosonic case considering a massless fermion, $M_f = 0$. To compare these results, we need the same arbitrary energy scale for both cases. We call this energy scale M .

Figures 1, 2 show the differential cross section for the massless boson and fermion for two cases $\phi = \pi/5$ and $\phi = \pi/100$ with $C = 0.01M^{-1}$, choosing $D = 0.01M^{-1}$ and also the special case where there is no draining, in the absence of the black hole. As can be seen, the result for the fermionic case tends to the bosonic one for small angles. Besides that, the left graphs in Figs. 1 and 2 show that for the limit $\omega \rightarrow 0$ the differential cross section for the spinor field goes to a nonzero constant in contrast with the boson field. To see this more closely let us expand Eq. (38) for small ω where $\alpha > \beta + \gamma^2$, which is the case for the graphs in Figs. 1 and 2, as

$$\frac{d\sigma_{\alpha>\beta+\gamma^2}}{d\phi} = \frac{C\pi}{2} - \frac{1}{2} \left(C^{3/2} \pi \cot(\phi/2) \right) \sqrt{\omega} + \mathcal{O}[\omega]. \quad (43)$$

As can be seen, in the limit $\omega \rightarrow 0$, the scattering cross section is equal to $C\pi/2$ for the fermion case which is only dependent on the circulation. We think this happens due to the fact that the fermionic field has an intrinsic angular momentum which interacts with the angular momentum of the black hole originating from the circulation.

4 Conclusion

In this paper, we have studied the differential cross section of a massive spinor field in the background of the acoustic black hole spacetime, as a toy model for the gravitational rotating black hole, using the partial wave approach. We have investigated the scattering of planar waves in a fermionic system by a background vortex as an analog for a rotating black hole. Because of the form of the spinor field which has upper and lower components, we have calculated the phase shifts for these components separately and then averaged them. We have worked with three dimensionless parameters α , β and γ related to the circulation, fermion mass and draining, respectively. We have obtained the differential cross section at long wavelengths and discussed the limiting cases including small angles and also in the absence of the circulation. One could see that the dominant contribution in the small angle limit for the fermionic case is exactly the same as the bosonic one when the mass of the fermion is zero. This dominant contribution comes from the circulation term. Therefore, for small angles the contribution of the circulation is more important than the draining one. Furthermore, considering the cross section in the absence of the circulation shows that the result is the same for the bosonic and fermionic cases when the fermion is massless. In this limit, the result is independent of the angle ϕ . The reason for that is in the absence of the circulation the only term that contributes in the long wavelength regime to the differential cross section is a polar symmetric term. Finally, we have shown that in contrast with the bosonic case in the limit $\omega \rightarrow 0$, considering $\alpha > \beta + \gamma^2$, the scattering cross section goes to a nonzero constant equal to $C\pi/2$ for the fermion case which is only dependent on the circulation.

The similar scattering behavior for both boson and fermion for small angles seems to be in accord with both being scattered between the horizon and the ergosphere radius. At this regime both enjoys the Penrose effect of gaining energy after the scattering (the superresonance effect). As Figs. 1, 2 (right panel) show, this indeed agrees with the increasing of the differential cross section as the frequency increases. This precisely happens as long as the fre-

quency belongs the interval $0 < \omega < m\Omega_H$, where m is the azimuthal mode number and Ω_H is the angular velocity of the black hole [36, 37, 66–68]. On the other hand, for large angles, both particles tend to be scattered outside the ergoregion and in turn they almost keep the scattering constant as Figs. 1 and 2 (left panel) show. This is particularly more accurate for fermions. A detailed analysis of the superresonance effect for fermion fields should be addressed elsewhere. Besides that, in a future work, we plan to study a more realistic model considering the dynamics of the fermionic fields interacting with a black hole, gravitational or as an analog in a condensed matter system.

Acknowledgements We would like to thank CNPq and CAPES for partial financial support. A. M. thanks PNPd/CAPES for the financial support.

Open Access This article is distributed under the terms of the Creative Commons Attribution 4.0 International License (<http://creativecommons.org/licenses/by/4.0/>), which permits unrestricted use, distribution, and reproduction in any medium, provided you give appropriate credit to the original author(s) and the source, provide a link to the Creative Commons license, and indicate if changes were made. Funded by SCOAP³.

References

1. W. Unruh, Phys. Rev. Lett. **46**, 1351 (1981)
2. W. Unruh, Phys. Rev. D **51**, 2827 (1995)
3. M. Visser, Class. Quantum Gravity **15**, 1767 (1998)
4. G. Volovik, *The Universe in a Helium Droplet* (Oxford University Press, Oxford, 2003)
5. L.C.B. Crispino, A. Higuchi, G.E.A. Matsas, Rev. Mod. Phys. **80**, 787 (2008)
6. M. Cadoni, S. Mignemi, Phys. Rev. D **72**, 084012 (2005)
7. M. Cadoni, Class. Quantum Gravity **22**, 409 (2005)
8. L.C. Garcia de Andrade, Phys. Rev. D **70**, 64004 (2004)
9. T.K. Das, Transonic black hole accretion as analogue system. [arXiv:gr-qc/0411006](https://arxiv.org/abs/gr-qc/0411006)
10. G. Chapline, P.O. Mazur, Superfluid picture for rotating spacetimes. [arXiv:gr-qc/0407033](https://arxiv.org/abs/gr-qc/0407033)
11. O.K. Pashaev, J.-H. Lee, Theor. Math. Phys. **127**, 779 (2001)
12. S. E. Perez Bergliaffa, K. Hibberd, M. Stone, M. Visser, Phys. D **191**, 121 (2004)
13. S.W. Kim, W.T. Kim, J.J. Oh, Phys. Lett. B **608**, 10 (2005)
14. X.-H. Ge, S.-F. Wu, Y. Wang, G.-H. Yang, Y.-G. Shen, Int. J. Mod. Phys. D **21**, 1250038 (2012)
15. C. Barcelo, S. Liberati, M. Visser, Living Rev. Rel. **8**, 12 (2005)
16. E. Berti, V. Cardoso, J.P.S. Lemos, Phys. Rev. D **70**, 124006 (2004)
17. V. Cardoso, J.P.S. Lemos, S. Yoshida, Phys. Rev. D **70**, 124032 (2004)
18. P.A. Horvathy, M.S. Plyushchay, Phys. Lett. B **595**, 547 (2004)
19. M.A. Cuyubamba, Class. Quantum Gravity **30**, 195005 (2013)
20. R. Schützhold, W.G. Unruh, Phys. Rev. D **66**, 044019 (2002)
21. G. Rousseaux, C. Mathis, P. Maïssa, T.G. Philbin, U. Leonhardt, New J. Phys. **10**, 053015 (2008)
22. U. Leonhardt, P. Piwnicki, Phys. Rev. Lett. **84**, 822 (2000)
23. U. Leonhardt, Nature **415**, 406 (2002)
24. W.G. Unruh, R. Schützhold, Phys. Rev. D **68**, 024008 (2003)
25. T.G. Philbin, C. Kuklewicz, S. Robertson, S. Hill, F. König, U. Leonhardt, Science **319**, 1367 (2008)

26. R. Schützhold, W.G. Unruh, Phys. Rev. Lett. **95**, 031301 (2005)
27. M. Novello, M. Visser, G. Volovik (eds.), *Artificial Black Holes* (World Scientific, Singapore, 2002)
28. L.J. Garay, J.R. Anglin, J.I. Cirac, P. Zoller, Phys. Rev. Lett. **85**, 4643 (2000)
29. O. Lahav, A. Itah, A. Blumkin, C. Gordon, J. Steinhauer, [arXiv:0906.1337](https://arxiv.org/abs/0906.1337)
30. S. Giovanazzi, Phys. Rev. Lett. **94**, 061302 (2005)
31. X.-H. Ge, S.-J. Sin, JHEP **1006**, 087 (2010)
32. N. Bilic, Class. Quantum Gravity **16**, 3953 (1999)
33. S. Fagnocchi, S. Finazzi, S. Liberati, M. Kormos, A. Trombettoni, New J. Phys. **12**, 095012 (2010)
34. M. Visser, C. Molina-Paris, New J. Phys. **12**, 095014 (2010)
35. M.A. Anacleto, F.A. Brito, E. Passos, Phys. Rev. D **85**, 025013 (2012)
36. M.A. Anacleto, F.A. Brito, E. Passos, Phys. Lett. B **703**, 609 (2011)
37. M.A. Anacleto, F.A. Brito, E. Passos, Phys. Lett. B **694**, 149 (2010)
38. B. Zhang, Thermodynamics of acoustic black holes in two dimensions. [arXiv:1606.00693](https://arxiv.org/abs/1606.00693) [hep-th]
39. H. Velten, D.J. Schwarz, J.C. Fabris, W. Zimdahl, Phys. Rev. D **88**, 103522 (2013)
40. A.M. Oliveira, H.E.S. Velten, J.C. Fabris, I.G. Salako, Eur. Phys. J. C **74**, 3170 (2014)
41. J.C. Fabris, O.F. Piattella, I.G. Salako, J. Tossa, H.E.S. Velten, Mod. Phys. Lett. A **28**, 1350169 (2013)
42. I.G. Salako, A. Jawad, [arXiv:1503.08714](https://arxiv.org/abs/1503.08714)
43. Y. Aharonov, D. Bohm, Phys. Rev. **115**, 485 (1959)
44. A. Tonomura, Phys. Rev. Lett. **48**, 1443 (1983)
45. M. Peskin, A. Tonomura, *The Quantum Hall Effect* (Springer, Berlin, 1989)
46. O. Bergman, G. Lozano, Ann. Phys. **229**, 416 (1994)
47. M.A. Anacleto, M. Gomes, A.J. da Silva, D. Spehler, Phys. Rev. D **70**, 085005 (2004)
48. M.A. Anacleto, M. Gomes, A.J. da Silva, D. Spehler, Phys. Rev. D **70**, 129905 (2004)
49. M.A. Anacleto, M. Gomes, A.J. da Silva, D. Spehler, Phys. Rev. D **71**, 107701 (2005)
50. M.A. Anacleto, J.R. Nascimento, A.Y. Petrov, Phys. Lett. B **637**, 344 (2006)
51. M.A. Anacleto, Phys. Rev. D **92**, 085035 (2015)
52. L.H. Ford, A. Vilenkin, J. Phys. A **14**, 2353 (1981)
53. V.B. Bezerra, Phys. Rev. D **35**, 2031 (1987)
54. V.B. Bezerra, J. Math. Phys. **30**, 2895 (1989)
55. G.A. Marques, V.B. Bezerra, Mod. Phys. Lett. A **19**, 49 (2004)
56. V.B. Bezerra, G.A. Marques, S.G. Fernandes, J. Math. Phys. **47**, 072504 (2006)
57. M.V. Berry, R.G. Chambers, M.D. Large, C. Upstill, J.C. Walmsley, Eur. J. Phys. **1**, 154 (1980)
58. E. Cerda, F. Lund, Phys. Rev. Lett. **70**, 3896 (1993)
59. C. Coste, F. Lund, M. Umeki, Phys. Rev. E **60**, 4908 (1999)
60. F. Vivanco, F. Melo, C. Coste, F. Lund, Phys. Rev. Lett. **83**, 1966 (1999)
61. D. Neshev, A. Nepomnyashchy, Y.S. Kivshar, Phys. Rev. Lett. **87**, 043901 (2001)
62. U. Leonhardt, P. Ohberg, Phys. Rev. A **67**, 053616 (2003)
63. M. Stone, Phys. Rev. B **61**, 11780 (2000)
64. S.R. Dolan, E.S. Oliveira, L.C.B. Crispino, Phys. Lett. B **701**, 485 (2011)
65. A.L. Fetter, Phys. Rev. **136**, A1488 (1964)
66. M.A. Anacleto, F.A. Brito, E. Passos, Phys. Rev. D **86**, 125015 (2012)
67. M.A. Anacleto, F.A. Brito, E. Passos, Phys. Rev. D **87**, 125015 (2013)
68. M.A. Anacleto, F.A. Brito, E. Passos, Phys. Lett. B **743**, 184 (2015)
69. D. Bazeia, R. Menezes, Phys. Rev. D **73**, 065015 (2006)
70. A. de Souza Dutra, M. Hott, F.A. Barone, Phys. Rev. D **74**, 085030 (2006)
71. D. Bazeia, M.M. Ferreira Jr., A.R. Gomes, R. Menezes, Phys. D **239**, 942 (2010)
72. A. de Souza Dutra, R.A.C. Correa, Phys. Rev. D **83**, 105007 (2011)
73. P.R.S. Carvalho, Phys. Lett. B **726**, 850 (2013)
74. R.A.C. Correa, R. da Rocha, A. de Souza Dutra, Ann. Phys. **359**, 198 (2015)
75. R.A.C. Correa, R. da Rocha, A. de Souza Dutra, Phys. Rev. D **91**, 125021 (2015)
76. I. Sakalli, M. Halilsoy, Phys. Rev. D **69**, 124012 (2004)
77. D. Lohiya, Phys. Rev. D **30**, 1194 (1984)
78. L. Nakonieczny, M. Rogatko, Phys. Rev. D **84**, 044029 (2011)